IOP Conference Series: Materials Science and Engineering

PAPER • **OPEN ACCESS**

Kinetic analysis of co-pyrolysis of biomass/sorbent mixtures at different ratios

To cite this article: A R Ariffen and N Yusoff 2020 *IOP Conf. Ser.: Mater. Sci. Eng.* **778** 012117

Kinetic analysis of co-pyrolysis of biomass/sorbent mixtures at different ratios

A R Ariffen[1] and N Yusoff[1]*

[1] School of Engineering and Physical Science, Heriot-Watt University Malaysia, 62200 Putrajaya, Malaysia

*Corresponding author: N.Yusoff@hw.ac.uk

Abstract. Biomass is one of the most promising sources of renewable energy. Gasification of carbonaceous and lignocellulosic biomasses produces gases, which can be upgraded as a clean feedstock for power plants. However, control and optimization of industrial gasification is still a challenging task due to a lack of understanding in solid state reaction mechanisms. This work attempts to improve kinetic modelling of a gasification process through analyses of four locally available biomasses, namely, oil palm trunk, fronds, empty fruit bunches, and coconut fibre. The biomasses were mixed with sorbents to enhance the pyrolysis and gasification reaction in a thermogravimetric analyser. In addition to common sorbents such as oxides of magnesium and calcium, two other sorbents, namely, rice husk and eggshell (a source of calcium carbonate) were blended at different ratios of biomasses to investigate their behaviour under pyrolytic decomposition conditions. Activation energies of the mixtures were obtained with the Reaction Rate Constant Model (RRCM). It was found that the mixtures had higher activation energies as compared to pure biomasses. For example, oil palm trunk without sorbent and with 50 wt% calcium oxide had activation energies of 26.87 and 46.83 kJ/mol, respectively. Majority of the sorbents also increased the thermal stability of the biomasses by increasing the mixtures' resistance to weight loss under high temperature. However, rice husk reduced the mixtures' thermal stability when compared with pure biomasses as evident in the oil palm trunk case when the mixture became 6.2% less thermally stable.

Introduction

Countries across the globe recognized the benefits of employing biomass as energy source and have taken actions to create better incentives through policy-making. Several countries in the European Union have set targets for bio-energy and in 2010, almost 10% of the energy supply in the EU was from biomass (1). The drive towards renewable energy is not limited to Europe for example, the government of Malaysia has been aiding and promoting the use of renewable energy sources, targeting to produce 11% of all electricity from renewable and environmentally friendly sources (2). Countries such as Malaysia and Indonesia have an abundant source of biomass due to its tropical nature; an example would be the two countries' palm oil industry. Malaysia and Indonesia respectively contribute to 41% and 44% of global oil palm production (3).

The by-products of oil palm related productions are an example of biomass. Oil palm industries process the fruits to extract its oil which accounts for 10% of the entire tree; the bulk 90% of the trees are left to decompose. In the process of extracting the palm oil during milling activities, the wastes generated are the empty fruit bunches, mesocarp fibers, kernel shells, and mill effluent whereas during plantation the wastes are the fronds and trunks.

Other biomass such as coconuts and rice husks are also abundant in Malaysia's landfills. Coconuts, for example, are used to produce milk by extracting the flesh; another one of its uses is coconut oil. Once the coconuts are grated, the solid wastes produced still have up to 24 wt% oil within them. With roughly 115,000 ha. of coconut plantation in Malaysia, the coconut milk and coconut oil industries produced 78,000 metric tons of solid waste in 2010 which were used as biomass, fertilizers, or animal feeds (4).

Rice is considered a staple food in Malaysia, with an average consumption of two and a half plates per day per person (5). With increasing population, rice consumption will inevitably increase with it; this will in turn increase the production and import of rice in the country. Alongside the increased consumption, production, and import of rice, there will be an increase in rice husk biomass wastes due

to the milling processes of rice; 78 wt% of rice are bran and broken rice whilst the remaining 22 wt% are rice husks (6).

Malaysia alone produces biomass wastes in abundance and will continue to do so as the population increases through time. As landfills are being filled with biomass wastes, it provided the scientific community to conjure a solution in utilizing the waste to convert into energy. One method of converting biomass into usable energy source is gasification whereas the carbonaceous fuels (biomass) is converted into combustible gases. The process produces syngas, namely hydrogen (H2), carbon dioxide (CO2), carbon monoxide (CO), methane (CH4), nitrogen (N2), and water vapor (H2O). By-products include tars, higher hydrocarbons, hydrogen sulphide (H2S), hydrogen chloride (HCl), and ammonia (NH3) (7).

Gasification can be divided into four steps: heating, drying, pyrolysis, and gasification. Pyrolysis is when the organic contents of the biomass fuels are irreversibly converted into gases, coke, and condensable water vapor (8). Temperature at which pyrolysis, also known as devolatilization, occurs is 300-650 °C whereas gasification occurs at higher temperatures ranging from 800-1000 °C (9). Pyrolysis is also a better alternative to agricultural waste burning because at the right conditions, biomass wastes will be converted into biochar; which is a solid residue of biomass pyrolysis where some carbon content is retained rather than released into the atmosphere.

This paper aims to investigate the kinetic parameters of biomass in the pyrolysis regime of the gasification process. The end results may provide an incentive on more efficient burning and ultimately enhancing the gasification process. Four biomasses, namely, empty fruit bunches (EFB), oil palm fronds (OPF), oil palm trunks (OPT), and coconut fibres (CF) were chosen to undergo kinetic analysis in thermogravimetric analysis (TGA). The biomass were premixed with different sorbents, namely, Calcium Oxide CaO, Calcium Carbonate CaCO3 (procured from eggshells), rice husks (RH), and Magnesium Oxide MgO at different weight ratios. The effects of the sorbents added into the biomasses at different ratios were studied to evaluate their thermal stabilities and activation energies.

Methodology

Taguchi method with L9 orthogonal array was selected as an experimental design approach. With 2 parameters containing 4 factors each and 1 parameter with 3 factors, the total number of samples needed to be analyzed was 36. Each biomass sample contained two different weight ratios of sorbent. The sequence of EFB analysis (Case A) are shown in Table 1. The sequence is repeated for OPF (Case B), OPT (Case C) and CF (Case D).

Table 1: TGA samples set-up based on Taguchi Method

Run No.	Biomass	Sorbent	Mixing Ratio (Biomass: Sorbent)
1	EFB	-	100:0
2	EFB	CaO	75:25
3	EFB	CaO	50:50
4	EFB	$CaCO_3$	75:25
5	EFB	$CaCO_3$	50:50
6	EFB	MgO	75:25
7	EFB	MgO	50:50
8	EFB	Rice Husk	75:25
9	EFB	Rice Husk	50:50
…	…	…	…

To replicate pyrolysis conditions in the TGA, the biomass/sorbent samples were placed in 70 µL alumina oxide crucible and then placed into the TGA. A 5-mg sample was preferred due to the highly sensitive weighing scale fitted into the TGA. The heating rate was set at 20 °C/min and the samples were heated from 25 to 900 °C. In addition to heating, purified nitrogen gas was injected into the TGA at 20 mL/min.

Reaction Rate Constant Method (RRCM) was used to determine the kinetic parameters of the biomass/sorbent mixtures at different weight ratios. RRCM does not rely on different heating rates to obtain the plots necessary to calculate the activation energies of the mixtures. Furthermore, numerous

studies have used RRCM in the study of biomass pyrolysis (10), (11), (12). For RRCM to be applicable, it was assumed that pyrolytic decomposition of biomass exhibits an innumerably large set of first order reactions; thus, enabling for the calculation of apparent activation energy at an overall first order reaction. This assumption was applied to represent the simultaneous reactions occurring during biomass pyrolysis and with an accepted degree of linearity from the Arrhenius plots.

Arrhenius equation with the assumption of overall first order reaction and as a function of mass loss is presented in Equation 1.

$$\frac{dX(t)}{dt} = k(1 - X(t)) \tag{1}$$

where $X(t)$ represents the conversion of the biomass sample at any given time t. Replacing t with sample temperature T and rearranging Equation 1 results in Equation 2. Integrating X with respect to T, a modified Equation 3 (natural log of the rate constant k against $1/T$) can be applied to plot the Arrhenius curves.

$$k = \beta \frac{dX(T)}{dT} / (1 - X(T)) \tag{2}$$

$$k = \frac{\beta[-\ln(|X(T_2) - 1|) + \ln(|X(T_1) - 1|)]}{T_2 - T_1} \tag{3}$$

Activation energies at different temperature regimes can be determined from the linear slopes of two points multiplied by a negative value of the universal gas constant R.

Results and Discussion

Thermal Stability

The mass loss profile of each biomass/sorbent sample was determined by using the TGA and was plotted as a function of temperature. The key features of the curves were their general trends and their corresponding temperatures. In addition to that, the transition between one weight loss regime to another was also monitored.

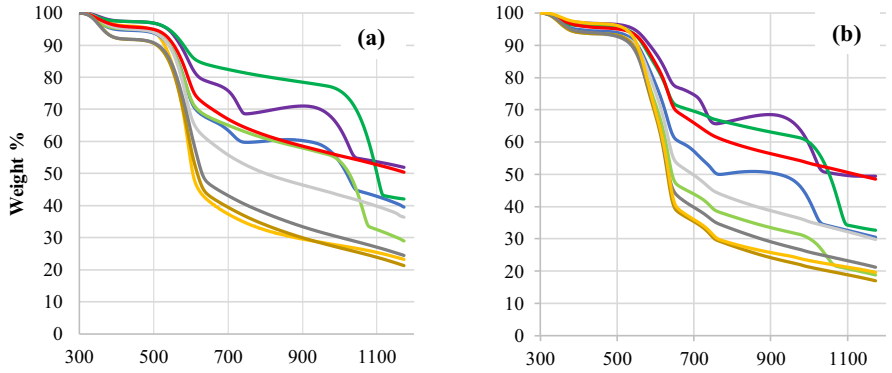

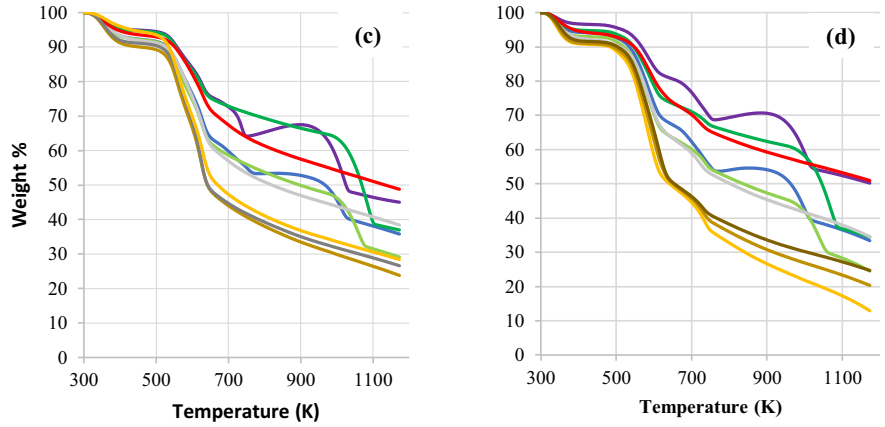

Figure 1 TGA curves of (a) EFB, (b) OPF, (c) OPT, (d) CF for Runs 1-9 for each case

Figure 1 shows the TGA curves of EFB, OPF, OPT, and CF, and also with their respective sorbent mixtures at different weight ratios. The first drop in weight percentage occurring up to 400 K was attributed to weight loss of moisture, the mixtures' weight then proceeded to be constant until 520 K. From 520 K onwards, there was a general decrease in weight percentage due to devolatilization, a process in which the biomass thermochemical conversion was initiated. Anomalies were observed for biomass mixtures with CaO as they showcased weight increase from 710-1080 K.

In Figure 1a, the TGA curve of pure EFB biomass showcased the decomposition of hemicellulose from 510-605 K. This can be seen from the initial rapid drop of weight percentage in the curve. Similar trends were observed from the pure OPF, OPT, and CF curves. Each of the pure biomass curve exhibited an initial steady weight loss due to water vaporization, which followed by a rapid drop of weight due to decomposition of hemicellulose. From this analysis, it can be concluded that pure OPF had the highest volatiles content due to its largest drop in weight during decomposition of hemicellulose (3). Following the decomposition of hemicellulose was the decomposition of cellulose, occurring at higher temperatures. The weight loss rate was then relatively constant from 750 K onwards, signifying the decomposition of lignin which occurred throughout the entire devolatilization regions (13).

The TGA curves of the mixtures were consistent with the pure biomass curves in terms of pattern of weight loss, however, the biomass with CaO mixtures displayed an increase in weight with increasing temperature. In Figure 1a, the EFB and CaO mixtures exhibited weight increase from 730-940 K. Similar trends can be observed for the OPF, OPT, and CF mixtures with CaO in Figures 1(a), 1(b) and 1(c). An explanation for this phenomenon is the carbonation of CaO where CaO was reacted with CO_2 released from devolatilization to form $CaCO_3$ (14). The $CaCO_3$ produced may have increased the sample weights before it was decomposed again at temperatures beyond 940 K. The decomposition of $CaCO_3$ was related to the calcination of $CaCO_3$ into CaO and CO_2. The increase then decrease of sample mixtures with CaO can be attributed to the cycle of carbonation-calcination reaction where CaO reacted with CO_2 to create $CaCO_3$, and then at higher temperature, the $CaCO_3$ decomposed to CaO and CO_2. A study conducted with regards to the carbonation-calcination reaction cycle recorded temperatures of 850 °C (1123 K) and above (15), which disagreed with the findings in this paper. It is important to note that the literature studied pure CaO and $CaCO_3$ rather than a mixture with biomass; with that said, the mixture of the sorbents with biomass may have lowered the temperatures at which the carbonation-calcination reaction cycle occur.

Through the TGA curves, the thermal stabilities of each mixture can be ranked against one another to investigate which mixture provided the highest thermal stability to each respective biomass. A further quantitative analysis was done by calculating the final conversion of the samples. Thermal stability was defined as the molecule's resistance to decomposition at high temperatures; the higher the thermal stability of a molecule is, the higher the temperature needed for decomposition. Studies have shown that

the TGA is the most commonly used apparatus to investigate thermal stability of materials such as biomass, polymers, crystalline, etc. (16). Henceforth, the final conversion of each biomass/sorbent mixtures were calculated and ranked from lowest to highest; the lowest conversion after the TGA run exhibited highest thermal stability and the highest conversion exhibited lowest thermal stability. Equation 4 was used to calculate for the samples' final conversions.

$$X_f = \frac{w_0 - w_f}{w_0} \quad (4)$$

The results of the thermal stability of mixtures are presented in Table 2.

Table 2: Most and Least Thermally Stable Biomass and Biomass/Sorbent Mixtures.

Biomass	Conversion (Without Sorbent)	Most Thermally Stable Sorbent Mixture and Ratio	Conversion (With Sorbent)	Least Thermally Stable Sorbent Mixture and Ratio	Conversion (With Sorbent)
EFB	0.767	CaO (50:50)	0.481	RH (50:50)	0.787
OPF	0.802	CaO (50:50)	0.506	RH (75:25)	0.830
OPT	0.715	MgO (50:50)	0.512	RH (75:25)	0.762
CF	0.871	MgO (50:50)	0.490	CF (100:0)	0.871

It was evident that adding MgO and CaO at 50:50 weight ratio between the biomass and sorbent increased the thermal stability of the mixture. However, adding rice husk as a sorbent reduced the thermal stability of the mixtures with CF.

Amongst the pure biomass group, OPT was the most thermally stable, but amongst the mixtures, EFB:CaO (50:50) was the most thermally stable mixture. This was partly due to the cycle of carbonation-calcination reaction that occurred with CaO mixtures. The least thermally stable pure biomass sample was CF, which inherently was also the least thermally stable when compared to mixtures with RH. The addition of RH into the biomass samples lowered thermal stability, making the samples decompose relatively more easily.

Different thermal stability properties can be attributed to different applications, for example, the higher thermal stability mixtures can be used in a gasification reactor as they will resist decomposition at higher temperatures thus yielding more usable gases. The lower thermally stable mixtures can be burnt more easily in a way that fewer amounts of ash are formed. Agricultural wastes can be mixed with RH to provide more efficient burning. Thus, in this thermal stability analysis, both most and least thermally stable mixtures provided insights on end-use applications for both gasification and waste management. Addition of CaO to EFB and OPF in 50:50 weight ratio increased the thermal stability by 59.50% and 58.60%, whilst the addition of RH in 75:25 weight ratio decreased the thermal stability of EFB and OPF by 2.50% and 3.30%. Addition of MgO to OPT and CF increased the thermal stability by 39.70% and 77.60% whilst the addition of RH decreased OPT thermal stability by 6.20%. The decrease in thermal stability when compared to pure biomass samples were relatively small in comparison with the increase in thermal stability with the addition of CaO and MgO.

Kinetic Parameters via DTG Temperature Regimes

The activation energies and pre-exponential factors of the biomass/sorbent mixtures were obtained using the RRCM. Initially, the activation energies of each peak temperature regimes were calculated to determine the minimum energy needed to initiate the decomposition of hemicellulose and cellulose. Temperature peaks were classified as a maximum mass loss rate surrounded by two minimums; the peaks were obtained by plotting derivative thermogravimetric (DTG) plots. The activation energies can then be determined by finding the slope of the Arrhenius curves from the corresponding temperatures in the temperature regime. This section will only focus on the kinetic analysis of the most thermally stable mixtures.

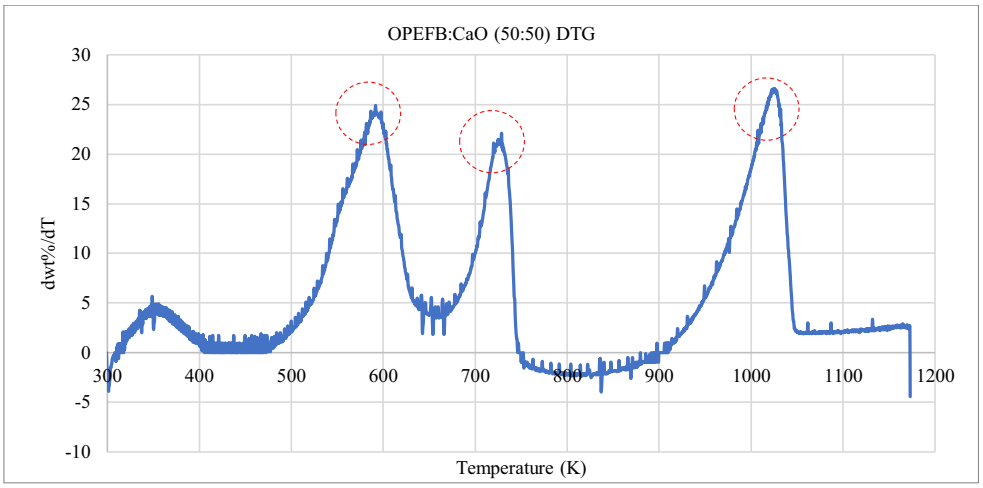

Figure 2: EFB: CaO DTG Curve to Determine Temperature Regimes.

The EFB:CaO DTG curve showcased three distinct temperature peaks: at 596 K, 725 K, and 1025 K. The initial temperature peak at 350 K was attributed to the vaporization of water and the kinetic analysis will focus mainly on the devolatilization processes. As mentioned earlier, a temperature regime is between two minimum mass loss rates with a peak mass loss rate in between. For EFB: CaO (50:50) mixture, the temperature regimes and its kinetic parameters are listed in Table 3.

Table 3: EFB: CaO (50:50) Kinetic Parameters at Different Temperature Regimes.

Temperature Range (K)		Activation	Pre-exponential	Weight
Start	**End**	**Energy (kJ/mol)**	**Factor (1/s)**	**Loss (%)**
458.667	658.667	-44.853	-0.0118	19.688
670.000	814.333	108.712	103.415	10.240
848.667	1113.333	-35.360	-33.930	24.204

Temperature regime ranging from 670-814 K was the only temperature regime to have a positive activation energy. The mass loss rate at this temperature was an indication of hemicellulose decomposition. Figure 2 indicated three mass loss regimes after the vaporization of water, which was also evident in raw data TGA curves different weight drop profiles were displayed.

Firstly, there is a gap in data entry (highlighted in dashed red circle), which related to the negative and zero values of k when Equation 8 was applied. Since the graph was plotted with ln(k) vs. 1/T, the ln of a negative and a zero gave invalid answers, the values were then removed from the plot to reduce noise. The oscillatory lines (highlighted in red circle) can be attributed to the difference in particle sizes between the biomass and sorbent.

Furthermore, certain regions of the Arrhenius plots exhibited positive slopes, which translated to negative activation energies. According to Table 3, two out of the three temperature regimes for the respective biomass/sorbent mixture had negative activation energies. When the mass loss rate decreases with increasing temperature, the corresponding Arrhenius curve changes its slope from negative to positive, hence the negative activation energy (17).

Pyrolysis of biomass, which is inherently heterogeneous, comprised of multiple dissociation reactions occurring simultaneously whilst a negative activation energy reaction suggested a two-step process in which one of them is spontaneous (negative) and the other is relatively small, making the overall activation energy negative. Since biomass pyrolysis is not a two-step process, there must be a different explanation for the apparent negative energy. Similar methods were applied to the rest of the most thermally stable mixtures of each biomass: OPF:CaO (50:50), OPT:MgO (50:50), and CF:MgO (50:50). The DTG curves of the mentioned biomass/sorbent mixtures can be found in Appendix A. The

Arrhenius plots of the mentioned biomass/sorbent mixtures can be found in Appendix B. Tables 4-6 provided a summary of the temperature regimes and their respective kinetic parameters.

Table 4: OPF: CaO (50:50) Kinetic Parameters at Different Temperature Regimes.

Temperature Range (K)		Apparent Activation	Pre-exponential	Weight Loss
Start	End	Energy (kJ/mol)	Factor (1/s)	(%)
455	666.667	-56.0615	-0.0148	20.825
670.667	781.667	136.0168	131.742	13.396
800	1110.667	-10.0818	-9.851	25.694

Table 5: OPT: MgO (50:50) Kinetic Parameters at Different Temperature Regimes.

Temperature Range (K)		Apparent Activation	Pre-exponential	Weight Loss
Start	End	Energy (kJ/mol)	Factor (1/s)	(%)
461.667	1171.667	47.749	7.514	47.761

Table 6: CF: MgO (50:50) Kinetic Parameters at Different Temperature Regimes.

Temperature Range (K)		Apparent Activation	Pre-exponential	Weight Loss
Start	End	Energy (kJ/mol)	Factor (1/s)	(%)
461.667	679.333	23.783	1.467	23.424
683.333	1012	9.905	-0.945	21.967

From Tables 4-6, only the biomass/sorbent mixtures with CaO exhibited negative apparent activation energies at their respective temperature regimes. Since this behaviour was not present in the MgO mixtures, the decrease in mass loss rate as temperature increases can be attributed to the carbonation-calcination cycle reaction in the CaO mixtures. The method of segregating the temperature regimes of each biomass/sorbent mixtures cannot provide the mixture's overall apparent activation energy, thus another method was applied.

Kinetic Parameters via Conversion

To obtain the kinetic parameters, namely the overall apparent activation energies and pre-exponential factors of each biomass/sorbent mixture, the activation energies of each mixture at conversions from 0.1-0.9 were interpolated through the Arrhenius plots. The activation energies at different conversions were then averaged to find the apparent overall activation energy for the respective mixtures.

The slopes of the Arrhenius curves were constantly changing, thus a small change in conversion lead to significant changes in activation energies. For example, based on the Arrhenius plot data for EFB, a conversion of 0.099799936 provided an activation energy of 62.99 kJ/mol whilst at conversion 0.100438993 the activation energy was 45.05 kJ/mol. A difference of about 0.0003 in terms of conversion changed the activation energy by -17.94 kJ/mol. In order to find the activation energy at conversion 0.1, for example, the slope between the upper and lower value of conversions were taken and interpolated. The calculation was then repeated for conversions 0.2-0.9. The apparent average activation energies were then plotted into bar charts to assess which biomass/sorbent mixture required the lowest activation energy.

Based on Figure 3(a), EFB:MgO mixture at 50:50 weight ratio had the highest apparent overall activation energy at 805.54 kJ/mol. The lowest apparent activation energy displayed in Figure 3(a) were the mixtures with RH, both were -16.82 kJ/mol at 75:25 weight ratio and -252.74 kJ/mol at 50:50 weight ratio. The two mixtures were the lowest in activation energy due to their negative values, the activation values were disregarded as the phenomenon of negative activation energies were not explored in this study. The mixtures with the lowest activation energies were EFB:CaO mixtures at both weight ratios: specifically, with 36.09 kJ/mol at 75:25 weight ratio and 69.47 kJ/mol at 50:50 weight ratio.

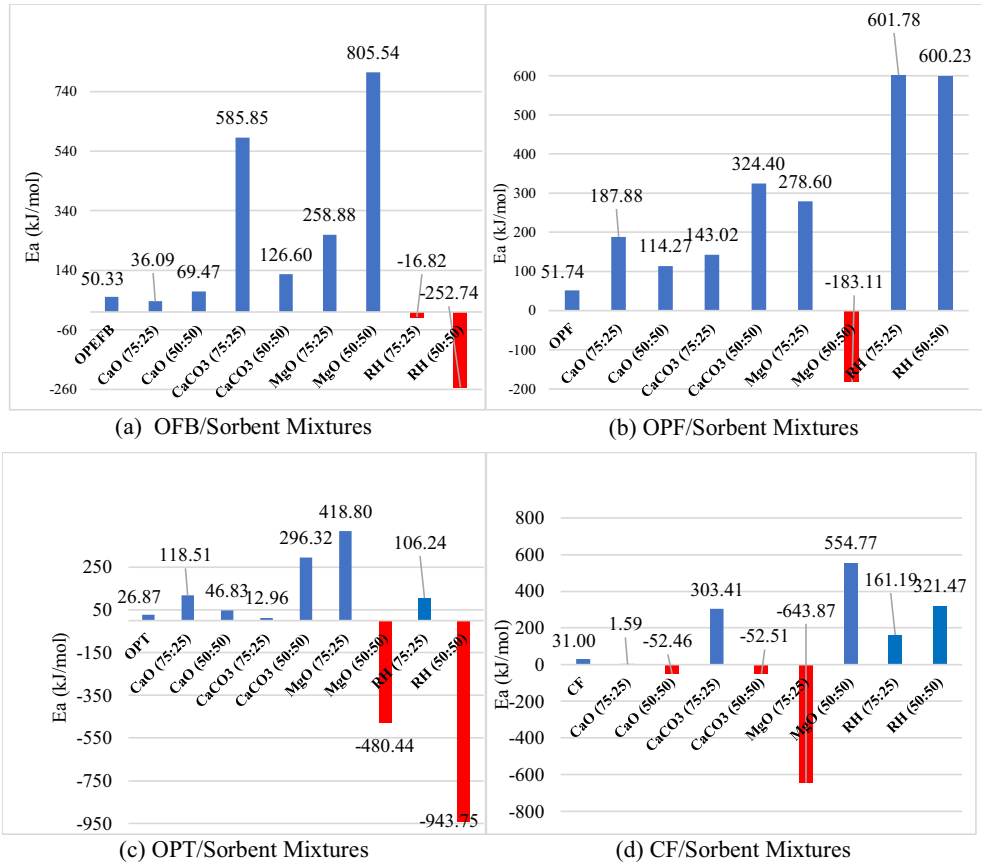

Figure 3: Biomass/Sorbent Mixtures at Different Weight Ratios and Their Respective Apparent Activation Energy, Ea.

Figures 3(b-d) showcased the apparent overall activation energies for each biomass and their respective blends at different weight ratios. The red bars are negative activation energies and thus will be disregarded in further discussions. For the OPF/Sorbent mixtures, the lowest activation energies were pure OPF biomass at 51.74 kJ/mol and OPF:CaO at 50:50 weight ratio with 114.27 kJ/mol. Pure OPT biomass' apparent activation energy was 26.87 kJ/mol When mixed with $CaCO_3$ at 75:25 ratio, the activation energy was 12.96 kJ/mol and with CaO at 50:50 weight ratio the activation energy was 46.83 kJ/mol, respectively. For CF, the pure biomass has an apparent activation energy of 31.00 kJ/mol and the lowest one was with CaO mixture at 75:25 weight ratio, with activation energy of 1.59 kJ/mol. For relevant analysis, the activation energies of the most stable biomass/sorbent ratios are listed in Table 7.

Table 7: Most Thermally Stable Biomass/Sorbent Mixtures and Their Respective Activation Energies.

Most Thermally Stable Biomass/Sorbent Mixture	Activation Energy (kJ/mol)
EFB: CaO (50:50)	69.47
OPF: CaO (50:50)	114.27
OPT: MgO (50:50)	-480.44
OPT: CaO (50:50)	46.83
CF: MgO (50:50)	554.77

Two mixtures were listed as most thermally stable for OPT due to the negative activation energy observed for OPT:MgO (50:50), thus the second most thermally stable mixture for OPT was taken. Table 7 essentially shows the most thermally stable mixtures of each biomass and at which weight ratios, also their respective activation energies.

Conclusions and Recommendations

The thermal stability of EFB, OPF, OPT, and CF with sorbent mixtures at different weight ratios were determined through TGA. Data provided were the weight loss percentage through temperature and with such data, a weight loss profile of each mixture was plotted. Thermal stability was determined by calculating each mixture's conversion; the lowest conversion was attributed to the highest thermal stability due to its high resistance to decomposition at high temperatures. It was found that CaO mixed with EFB and OPF at 50:50 weight ratio were the most thermally stable mixtures, increasing it by 59.50% and 58.60% when compared to pure EFB and OPF biomass. Addition of MgO to OPT and CF at 50:50 weight ratio increased the biomass' thermal stability by 77.60% and 39.70%.

Overall, addition of CaO and MgO increased the biomass' thermal stability significantly. This property can influence gasification performances as a more thermally stable mixture decomposes at a slower rate and may produce more useable gases. The solid residues formed from pyrolysis such as biochar may provide for further end-use application due to the remaining carbon content within.

Reaction rate constant method (RRCM) was used to determine the average apparent activation energies of the most thermally stable mixtures of each biomass. The average apparent activation energy was calculated by averaging the apparent activation energies of each mixture at conversions 0.1-0.9. The average apparent activation energies were 69.47, 114.25, 46.83, and 554.77 kJ/mol for EFB:CaO (50:50), OPF:CaO (50:50), OPT:CaO (50:50), and CF:MgO (50:50) respectively. The addition of sorbents did not just increase the thermal stability of the biomass, it also increased the activation energy.

A disadvantage of RRCM is that it did not provide a constant activation energy throughout the entire pyrolysis reaction. It was observed that biomass pyrolysis exerted different mass loss rates at different temperature regimes, namely for the decomposition of hemicellulose, cellulose, and lignin. The transition between one temperature regime to another cannot be captured by RRCM and there can be between 2 and 20% mass lost between one temperature regime to another (17).

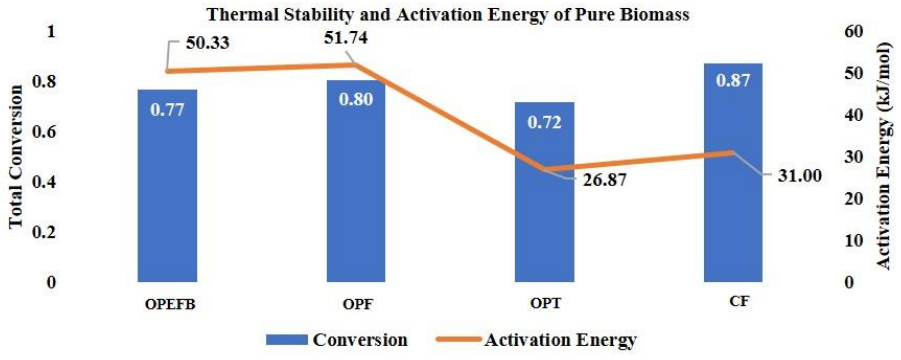

Figure 4: Thermal Stability and Activation Energy of Pure Biomass.

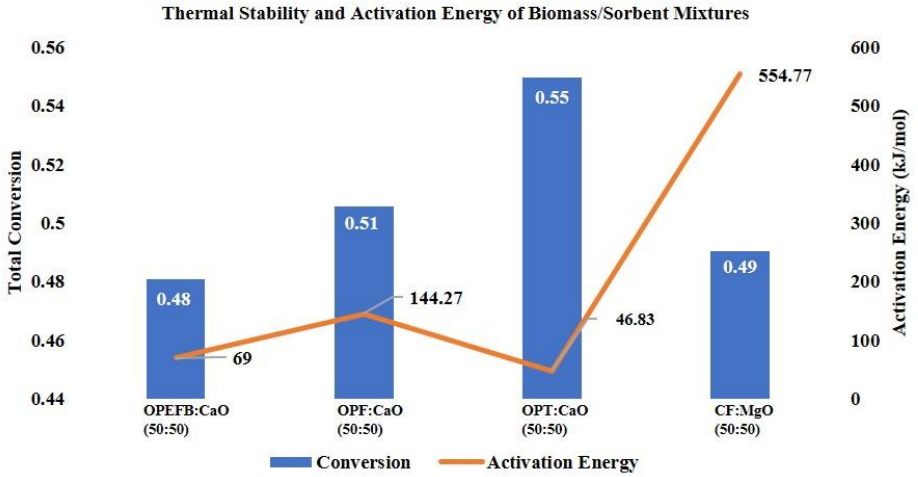

Figure 5: Thermal Stability and Activation Energy of the Most Thermally Stable Biomass/Sorbent Mixture.

The effects of sorbents on biomass can be seen in Figures 4 and 5. As the sorbents were added into the pure biomass samples in 50:50 weight ratio, the total conversion of the mixture drops, indicating higher thermal stability. At the same time, the activation energies of each mixture were increased, as indicated in the orange lines in Figures 4 and 5. Overall, the most thermally stable mixture with the lowest activation energy was EFB: CaO at 50:50 weight ratio; with an overall conversion of 0.48 and activation energy of 69.47 kJ/mol.

The thermal stability and kinetic parameter analysis of each biomass/sorbent mixture provided the information needed to enhance the pyrolysis reaction that occurs within gasification, so that the overall efficiency of the gasifier is increased. With this, agricultural wastes in Malaysia, namely oil palm and coconut biomass, can be mixed with CaO to improve pyrolysis performance and hence, the gasification process that follows; therefore, successfully converting wastes into usable gases for energy generation. It is important to note that the following experiments were done in lab conditions with numerous controlled variables such as the careful procedure of biomass preparation, whereas more factors must be considered to industrialize and commercialize said process. Small changes in selectivity and efficiency will significantly affect the overall performance of the gasification process.

For further studies, it was recommended to include other kinetic parameters method to calculate the activation energies. Other methods such as the Kissinger and Flynn-Wall Ozawa methods relied on different heating rates of the biomass/sorbent mixtures, thus an alteration of the experimental set-up is necessary. Implementation of different heating rates will also provide a better understanding of how the decomposition of each components (hemicellulose, cellulose, and lignin) behave with different weight ratios of sorbents added. To further investigate the negative activation energies discovered at certain temperature regimes obtained from the DTG temperature peaks, a quadrupole mass spectrometry can be used to monitor gas evolution. One study found that in the negative activation energy temperature regimes for corn stover and cocoa shell, there was an increase in evolution of CH_4 and C_2H_2 (17). A follow-up study on oil palm and coconut biomass wastes with sorbent mixtures at different weight ratios should be studied to investigate the types and amounts of gases evolved in the temperature regimes where activation energies were negative.

Acknowledgment
The authors wish to acknowledge Heriot-Watt University Malaysia (HWUM) for financial support and University Tenaga Nasional (UNITEN) for supplying several biomass samples used in this work. The authors also appreciate contributions by Heri Roziana Rusman (HWUM technician) for helping us with sample analyses using TGA.

References

[1] Khan Z, Yusup S, Ahmad MM, Uemura Y, Chok VS, Rashid U, et al. Kinetic Study on Palm Oil Waste Decomposition. *Biofuel's Engineering Process Technology*. 2011:523-36.
[2] Idris SS, Rahman NA, Ismail K. Combustion characteristics of Malaysian oil palm biomass, sub-bituminous coal and their respective blends via thermogravimetric analysis (TGA). *Bioresource Technology*. 2012:581-91.
[3] Onoja E, Chandren S, Razak FIA, Mahat NA, Wahab RA. Oil Palm (Elaeis guineensis) Biomass in Malaysia: The Present and Future. *Waste and Biomass Valorization*. 2018:1-20.
[4] Sulaiman S, Abdul Aziz AR, Aroua MK. Reactive extraction of solid coconut waste to produce biodiesel. *Taiwan Institute of Chemical Engineers*. 2012;**44**:233-8.
[5] Rajamoorthy Y, Abdul Rahim Kb, Munusamy S. Rice Industry in Malaysia: Challenges, Policies and Implications. *Procedia Economics and Finance*. 2015;**31**:861-7.
[6] Tambichik MA, Mohamad N, Samad AAA, Bosro MZM, Iman MA. Utilization of construction and agricultural waste in Malaysia for development of green concrete: a review. *Earth and Environmental Science*. 2018;**140**:1-9.
[7] Doherty W, Reynolds A, Kennedy D. Process simulation of biomass gasification integrated with a solid. *Journal of Power Sources*. 2015;**277**:292-303.
[8] Heidenreich S, Müller M, Foscolo PU. Fundamental Concepts in Biomass Gasification. *Advanced Biomass Gasification*. London: Elsevier; 2016. p. 4-10.
[9] Basu P. Pyrolysis. *Biomass Gasification, Pyrolysis and Torrefaction*. London: Elsevier; 2013. p. 147-76.
[10] Yangali P, Celaya AM, Goldfard JL. Co-pyrolysis reaction rates and activation energies of West Virginia coal and cherry pit blends. *Journal of Analytical and Applied Pyrolysis*. 2014;**108**:203-11.
[11] Celaya AM, Goldfarb JL. Models and Mechanisms to Explore the Global Oxidation Kinetics of Blends of feed corn stover and Illinois No. 6 Coal. *J Thermodyn Catal*. 2014;**5**(2):136.
[12] Li W, Xue Y, Cui Z. Size dependence of surface thermodynamic properties of nanoparticles and its determination method by reaction rate constant. *Physica B*. 2016;**495**:98-105.
[13] Mabuda AI, Mamphweli NS, Meyer EL. Model free kinetic analysis of biomass/sorbent blends for gasification purposes. Elsevier. 2015:1656-64.
[14] Abdul Halim Yun H, Dupont V. Thermodynamic analysis of methanation of palm empty fruit bunch (PEFB) pyrolysis oil with and without in situ CO2 sorption. *AIMS Energy*. 2015;**3**(4):774-97.
[15] Mohamed M, Yusup S, Bustam MA. Synthesis of CaO-based Sorbent from Biomass for CO2 Capture in Series of Calcination-carbonation Cycle. *Procedia Engineering*. 2016;**148**:78-85.
[16] Agag T, Geiger S, Ishida H. Chapter 13 - Thermal Properties Enhancement of Polybenzoxazines: The Role of Additional Non-Benzoxazine Polymerizable Groups. *Handbook of Benzoxazine Resings*. London: Elsevier; 2011. p. 263-86.
[17] Patnaik A, Goldfarb JL. Continuous Activation Energy Representation of the Arrhenius Equation for the Pyrolysis of Cellulosic Materials: Feed Corn Stover and Cocoa Shell Biomass. *Cellulose Chemistry and Technology*. 2015;**50**(2):311-20.